Hydrol. Earth Syst. Sci. Discuss., 7, 3365–3396, 2010
www.hydrol-earth-syst-sci-discuss.net/7/3365/2010/
doi:10.5194/hessd-7-3365-2010

Hydrology and Earth System Sciences Discussions

Estimation of surface soil moisture and roughness from multi-angular ASAR imagery in the Watershed Allied Telemetry Experimental Research (WATER)

S. G. Wang[1,2], **X. Li**[1], **X. J. Han**[1], **and R. Jin**[1]

[1]Cold and Arid Regions Environmental and Engineering Research Institute, Chinese Academy of Sciences, Lanzhou 730000, China
[2]Graduate University of Chinese Academy of Sciences, Beijing 100039, China

Received: 11 May 2010 – Accepted: 19 May 2010 – Published: 8 June 2010

Correspondence to: X. Li (lixin@lzb.ac.cn)

Published by Copernicus Publications on behalf of the European Geosciences Union.

Abstract

Radar remote sensing has demonstrated its applicability to the retrieval of basin-scale soil moisture. The mechanism of radar backscattering from soils is complicated and strongly influenced by surface roughness. Furthermore, retrieval of soil moisture using AIEM-like models is a classic example of the underdetermined problem due to a lack of credible known soil roughness distributions at a regional scale. Characterization of this roughness is therefore crucial for an accurate derivation of soil moisture based on backscattering models. This study aims to directly obtain surface roughness information along with soil moisture from multi-angular ASAR images. The method first used a semi-empirical relationship that connects the roughness slope (Zs) and the difference in backscattering coefficient ($\Delta\sigma$) from ASAR data in different incidence angles, in combination with an optimal calibration form consisting of two roughness parameters (the standard deviation of surface height and the correlation length), to estimate the roughness parameters. The deduced surface roughness was then used in the AIEM model for the retrieval of soil moisture. An evaluation of the proposed method was performed in a grassland site in the middle stream of the Heihe River Basin, where the Watershed Allied Telemetry Experimental Research (WATER) was taken place. It has demonstrated that the method is feasible to achieve reliable estimation of soil water content. The key challenge to surface soil moisture retrieval is the presence of vegetation cover, which significantly impacts the estimates of surface roughness and soil moisture.

1 Introduction

Surface soil moisture (mv) is important in agronomic, hydrological, and meteorological processes at all spatial scales. It plays a key role in water stress detection and irrigation management, especially for arid and semi-arid regions. The ability of inferring mv using both active and passive microwave techniques has been intensively demonstrated (Ulaby et al., 1982, 1986; Jackson et al., 1995, 2002; Njoku and Entekhabi, 1996; Su

HESSD

7, 3365–3396, 2010

et al., 1997; Kerr et al., 2001; Njoku et al., 2003; Wigneron et al., 2003, 2007; Moran et al., 2004; Baghdadi et al., 2008). It is well known that space-borne passive systems possess the advantage of high revisit capacity, however, the spatial resolution of passive microwave remote sensing is too coarse to be employed at the catchment scale. On the other hand, SAR sensors have the capability to provide finer spatial resolution, on the order of tens of meters, meeting most requirements for watershed management and hydrological applications.

Radar system emits pulses and receives echoes backscattered from the illuminated areas. The intensity value of each pixel is proportional to the radar backscattering coefficient, which depends on several factors, including the instrument's technical specifications (frequency and polarization), terrain, dielectric characteristics (ε_r; strongly related to the soil water content) and the geometrical structure (roughness) of the target surface.

Three categories of methods were developed to investigate the relationship between land surface properties and SAR observed backscattering coefficient (σ^0). The first kind is the theoretical scattering model, which was derived and employed to gain insight into the interaction of microwave propagation with natural surfaces based on physical laws, including the Kirchhoff approximation (KA), which consists of the geometrical optics model (GOM) and physical optics model (POM), the small perturbation model (SPM) (Ulaby et al., 1982), and the integral equation model (IEM) (Fung et al., 1992, 1994). Among these models, the IEM unites the KA and the SPM which was verified by laboratory measurements of bistatic scattering from surfaces with small, intermediate and large scale roughness. The advanced IEM (AIEM) improves the calculation accuracy of scattering coefficient by keeping the absolute phase term in Greens function which was neglected by IEM (Wu et al., 2001; Chen et al., 2003). In principle, the dielectric constant of the soil surface and hence the soil water content can be estimated from the mathematical inversion of these models with the requirement of some restrictive assumptions. The IEM and the AIEM were often used for bare or sparse vegetation soils.

HESSD
7, 3365–3396, 2010

In contrast, the second kind of method is the empirical approach, with little physics behind it. Traditionally, in situ field soil moisture measurements were used to calibrate the linear relationship between these observations and radar backscattering coefficients (Ulaby et al., 1986) and this type of connection was evolved with increasingly fruitful datasets (Holah et al., 2005; Baghdadi et al., 2006a). The linear expression is often given by Eqs. (1) or (2)

$$\sigma^0 = a(mv) + b \tag{1}$$

$$\sigma^0 = a(mv) + b(\text{roughness}) + c \tag{2}$$

where a, b, and c are empirical constants. More sophisticated empirical methods have been proposed as well, with varying degrees of success. For example, Oh et al. (1992, 2002) separated the individual effects of roughness, vegetation, topography, and soil moisture on radar response using multi-frequency and multi-polarization measurements. Dubois et al. (1995) delineated the contributions of all combinations of surface conditions (roughness and vegetation) and radar configurations (frequency, polarization, and incidence angle) to the co-polarized backscattering coefficients σ^0_{HH} and σ^0_{VV}. However, these empirical relationships are site-specific and may not be applicable to datasets other than those used for development (Dubois et al., 1995).

To circumvent this problem, semi-empirical backscattering models may be more useful in determination of land surface geophysical parameters including soil moisture which represent a compromise between the complexity of the theoretical models and the simplicity of empirical models. They are an improvement on empirical models as they start from a physical background and then use simulated or experimental data sets to simplify the theoretical backscattering models (Shi et al., 1997; Loew et al., 2006; D'Urso and Minacapilli, 2006; Zribi et al., 2006). The main advantage of these types of models is that they are robust, relatively simpler and not site dependent.

In IEM and AIEM, the surface roughness is essential an input, thus, if only a single configuration (e.g., one polarization, one frequency) of radar data is available, rough-

Discussion Paper | Discussion Paper | Discussion Paper | Discussion Paper |

HESSD

7, 3365–3396, 2010

Estimation of surface soil moisture and roughness

S. G. Wang et al.

ness parameters should be known as a priori information in order to retrieve soil moisture content using these models. Unfortunately, surface roughness measurement is very time-consuming and almost impractical at the regional scale, moreover, appreciable inaccuracies may occur due to various deployments of instrumentation, sampling strategy, and the ambiguous scale effect during field campaigns and data post-processing (Davidson et al., 2000; Bryant et al., 2007). Hence, it is critical to obtain appropriate physical model-dependent surface roughness information at remote-sensing spatial scales in the context of soil moisture inversion.

Generally speaking, surface roughness is statistically characterized by three parameters: the standard deviation of surface height (σ), the correlation length (*cl*), and the autocorrelation function type (*ACF*). From pixel to pixel, these three parameters vary markedly, and the significant influence of surface roughness on scattering properties still limits the ability to correctly infer *mv* values unless detailed roughness measurements or estimations are available (Zribi et al., 2005; Verhoest et al., 2008; Lievens et al., 2009). In recent years, some studies have focused on this issue in attempts to reduce the impact of surface roughness on *mv* derivation. Baghdadi et al. (2002, 2004, 2006b) empirically calibrated the IEM based on a large number of SAR images with diverse incidence angles, polarization configurations, and frequencies against in situ measurements to deduce an optimal *cl*. This method has been shown to be effective, wherein the reproduced backscatter has consistently agreed with measured data and the validity of the calibrating approach has been evaluated on other complementary test sites (Álvarez-Mozos et al., 2008). Zribi and Dechambre (2002) have discussed the merits of the multi-angular method for surface roughness estimation and proposed a *Zs*-index that integrates σ and *cl*, and revealed the backscattering coefficients difference between multi-angular images is very sensitive to the *Zs*-index. Rahman et al. (2007, 2008) have suggested other procedures to link radar backscatter to roughness parameters (σ and *cl*), and the strategy of retrieval was dependent on IEM and lookup tables (LUT) under dry soil conditions. The use of these procedures marks the beginning of the determination of both roughness parameters and the estimation of *mv*

HESSD
7, 3365–3396, 2010

via multi-angular radar images instead of using ancillary data.

The objective of this paper is to develop and evaluate an operational method that explores surface roughness based solely on multi-angle SAR data, and the estimated roughness could further be used in the backscatter models to retrieve water content in the surface soil layer. The strategy consists in a semi-empirical procedure deduced form AIEM simulations, in association with a calibrated form within σ and *cl* proposed by Baghdadi et al. (2006b), to estimate roughness parameters for each grid cell from multi-angular ASAR images. When σ and *cl* are obtained, soil moisture was then retrieved using the AIEM. This paper is organized into four sections. In Sect. 2, which follows the introduction, the proposed methodology, the study site, and the datasets are described. Section 3 presents the detailed application on estimating both surface roughness and soil moisture over the study area. Then, the retrieved results in terms of soil moisture are validated by in situ measurements and the error sources are analyzed. Finally, Sect. 4 gathers our conclusions.

2 Method and data

2.1 Backscattering model for vegetated rough surface

For a given incidence angle θ, the backscattering coefficient above canopy ($\sigma^0_{\mathrm{can}}(\theta)$, $\mathrm{m^2\,m^{-2}}$) can be expressed as

$$\sigma^0_{\mathrm{can}}(\theta) = \sigma^0_{\mathrm{veg}}(\theta) + \sigma^0_{\mathrm{veg+soil}}(\theta) + \gamma^2(\theta)\sigma^0_{\mathrm{soil}}(\theta) \tag{3}$$

where, the first term $\sigma^0_{\mathrm{veg}}(\theta)$ represents the backscattering from the vegetation canopy, the second term $\sigma^0_{\mathrm{veg+soil}}(\theta)$ represents the interaction between the vegetation layer and the soil underneath and accounts for multiple scattering effects, and the third term $\gamma^2(\theta)\sigma^0_{\mathrm{soil}}(\theta)$ represents the backscattering from the soil layer that is attenuated by the canopy. $\gamma^2(\theta)$ is the two-way vegetation transmissivity.

In this study, the backscattering from the vegetation canopy and the vegetation transmissivity are calculated using the water cloud model (Attema and Ulaby, 1978), wherein it is assumed that the vegetation-soil interactions can be neglected, thus, the corresponding terms in Eq. (3) can be expressed as

$$\sigma^0_{\text{veg}} = A\,\text{vwc}\cos(\theta)[1-\gamma^2(\theta)] \tag{4}$$

$$\gamma^2(\theta) = \exp[-2b\,\text{vwc}/\cos(\theta)] \tag{5}$$

where vwc represents the vegetation water content ($\text{kg}\,\text{m}^{-2}$). Parameters A and b depend on the vegetation type, growth conditions, and radar frequency.

The backscattering from the soil layer is calculated using the AIEM which is a physically based radiative transfer model and more applicable to a wider range of land surface conditions than IEM (Wu et al., 2001; Chen et al., 2003). The AIEM essentially quantifies (or simulates) the backscattering coefficient as a function of the sensor parameters, namely radar frequency, polarization and incidence angle; and the surface parameters, such as soil dielectric constant, roughness parameters σ, cl and the ACF.

In AIEM, the single scattering term is given by

$$\sigma^S_{pq} = \frac{k^2}{2}\exp[-(\sigma)^2(k_z^2+k_{sz}^2)]\sum_{n=1}^{\infty}(\sigma)^{2n}\left|I^n_{pq}\right|^2\frac{W^{(n)}(k_{sx}-k_x,k_{sy}-k_y)}{n!} \tag{6}$$

$$I^n_{pq} = (k_{sz}+k_z)^n f_{pq}\exp[-(\sigma)^2k_zk_{sz}] + \frac{(k_{sz})^nF_{pq}(-k_x,-k_y)+(k_z)^nF_{pq}(-k_{sx},-k_{sy})}{2} \tag{7}$$

with

$$k_x = k\sin\theta\cos\phi$$

$$k_y = k\sin\theta\sin\phi$$

$$k_z = k\cos\theta$$

HESSD

7, 3365–3396, 2010

Estimation of surface soil moisture and roughness

S. G. Wang et al.

$$k_{sx} = k\sin\theta_s\cos\phi_s$$

$$k_{sy} = k\sin\theta_s\sin\phi_s$$

$$k_{sz} = k\cos\theta_s$$

where k is the wave number, I_{pq}^{n} is a function of θ, ϕ, σ and ε_{r} (soil dielectric constant). $W^{(n)}$ is the Fourier transform of the nth power of the surface correlation function. The subscripts p and q indicate polarization state. θ and ϕ are zenith angle and azimuth angle of the sensor, θ_s and ϕ_s are zenith and azimuth of scattering angle, respectively. For dielectric constant of soil, the Dobson model is used (Dobson et al., 1985).

2.2 Inversion strategy for soil moisture

In SAR remote sensing applications, the sensor configurations are known, while the surface roughness and dielectric constant are unknown. Estimation of soil surface parameters was usually obtained by using theoretical models to convert the measured backscatter coefficient into soil surface roughness and moisture. In the current study, the first procedure of soil moisture inversion is to remove the vegetation effect, which can be implemented by using Eqs. (3) to (5). After that, if assuming the soil texture and the correlation function type, which can be easily measured in field and are less variable in space, are known as a priori information, three unknowns will be left in the above functions, those are *mv*, and roughness parameters σ and *cl*.

Generally speaking, for inversion of soil moisture, at least three independent backscattering observations are needed. Multi-frequency configuration onboard aircraft platform (Bindlish and Barros, 2000), multi-angular and multi-polarization observing ability of current satellite-borne SAR such as ASAR provides this a possibility. However, multi-angular observations are usually highly correlated. Therefore, to increase the stability of inversion for soil moisture, a two-step inversion strategy is employed in this paper. The first step, roughness parameters σ and *cl* are retrieved from multi-angular observations using some semi-empirical models, as described in Sect. 3.1.

HESSD
7, 3365–3396, 2010

The second step, soil moisture is estimated using an iterative least squares minimization algorithm, which minimize the difference between the observed and AIEM computed backscattering coefficient. The cost function is defined as

$$J = [\sigma^0_{\mathrm{obs}} - \sigma^0_{\mathrm{est}}(mv)]^2 \tag{8}$$

where σ^0_{obs} is the radar observation, $\sigma^0_{\mathrm{est}}(mv)$ represents the estimation obtained from the AIEM simulations and mv is the soil moisture that needs to be determined.

2.3 Study area

The study was carried out at one of the WATER experimental site. WATER is a simultaneous airborne, satellite-borne, and ground-based remote-sensing experiment taking place in the Heihe River Basin, the second largest inland river basin in an arid region of northwestern China (Li et al., 2009). One of the most important components of the WATER is the arid region hydrology experiment (ARHE). The goal of the ARHE, which is being carried out in the middle streams of the Heihe River Basin (Fig. 1), is to study water and energy cycles in arid regions.

The Linze grassland (LZG; 100°04′ E, 39°15′ N), which covers an area of 2×2 km^2, is located in Linze county, Zhangye city in the middle stream of the Heihe River basin (Fig. 1). It was selected as one of the foci experimental areas (FEAs) in ARHE and is the study area in this investigation. Land cover types are diverse in this region, with wetland, grassland, salinized land, and farmland distributed in the vicinity. During the field campaigns conducted in the intensive observation period (IOP) from May to August 2008, five experimental sites (ESs), each 360×360 m^2 in size, were established on different landscapes in this region (Fig. 2). Experimental sites B and C were covered with short and sparse grass, whereas site A was a dry reed field. Alfalfa and barley were planted at sites D and E, both of which are irrigated farmland. It should be noted that ESs A, B, and C were severely encrusted with salt and alkali materials, while site D also suffered to some extent from salinization.

2.4 Ground truth measurements

Ground truths, including soil moisture, land surface temperature (T), and bulk density, were concurrently collected at all five ESs with radar acquisitions. A three-level stratified sampling strategy, illustrated in Fig. 2, was designed to collect ground truths. FEAs, ESs, and elementary sampling plots (ESP) correspond to nested scales from coarse to finer resolutions. The ESP, which is embedded within each ES, covering an area of approximately $120 \times 120\,\text{m}^2$ in a grid pattern at 20 m spacing, is representative of the entire ES in which the soil samples were collected.

Concurrently with radar overpasses on 27 June 2008, ground measurements were carried out from 10:00 a.m. to 01:00 p.m. (Beijing Time) (within ±2 h of the satellite overpass) at every ESP. A portable global positioning system (GPS) was used to obtain the coordinates of each site. The moisture contents of sites D and E were measured by time domain reflectometry (TDR). The gravimetric sampling method was used at the other three ESs due to the strong salinization of these sites. Soil moisture was sampled for the topsoil layer (5 cm), which is assumed as the maximum penetration depth by ASAR, at a frequency of 5.3 GHz. Soil bulk density was measured in order to transform gravimetric content into volumetric soil moisture content. Soil texture was analyzed in the laboratory.

No rainfall was recorded in the time windows of the satellite acquisitions. In addition, surface roughness is assumed to depend only on tillage practice and to be invariant during these dates. The roughness was surveyed using a pin profilometer with a 1-m profile length at every sampling point. It should be mentioned that the roughness were not measured at sites D and E because the canopy at these sites hindered profilometry. Detailed sampling of soil moisture and roughness is summarized in Table 1 and other soil properties are summarized in Table 2.

As for the parameters used in the water cloud model, the vegetation water content was measured only at site E on 18 June 2008, which was the closest date when radar images for the same experimental area were collected. Due to insufficient measurements, the vwc at site D was inferred based on local situations. Constants A and b were not measurable, therefore, their estimations were mainly referred to Bindlish and Barros (2001). The values of vegetation parameters and the crop growth status are shown in Table 3.

2.5 Radar imagery

ASAR operates at the C-band (5.3 GHz) and was launched onboard ENVISAT in 2002. ASAR features enhanced capability in terms of coverage, with selectable incidence angles, polarizations, and operational mode configurations. In this investigation, three contiguous ASAR images at alternating polarization precision (APP) modes at different incidence angles ranging from IS1 to IS7 were acquired. The orbital information of processed images is presented in Table 4.

After calibration, the speckle noise in the images was filtered by a 5×5 enhanced Lee filter. Changes in the local incidence angle were not considered because the topography is flat in the study area. Geolocation was performed according to the UTM projection system using a Landsat ETM+ image as a reference. The registration error was within one pixel. Figure 3 illustrates the subsets of the processed images of the Linze grassland FEA.

3 Results and discussion

3.1 Mapping surface roughness and soil moisture

Zribi and Dechambre (2002) showed that, if all other parameters are kept constant, the difference in backscattering coefficient ($\Delta\sigma$, in dB) between two distinct incidence angles is proportional to the index of the roughness slope, Zs, which can be represented as

$$Zs = \sigma^2/cl \tag{9}$$

HESSD

7, 3365–3396, 2010

Estimation of surface soil moisture and roughness

S. G. Wang et al.

Through IEM simulations, it was found that *Zs* is linked to $\Delta\sigma$ via the following

$$\Delta\sigma_{\theta_1-\theta_2} = f(Zs) \tag{10}$$

The specific function needs to be obtained through statistical analysis. In our case, since the images with the incidence modes of IS1 and IS7 were acquired on successive dates (Table 4), we used these two images in HH polarization for analysis. A forward simulation using AIEM was carried out, with σ ranging from 0.3 to 3.0 cm and *cl* from 3 to 35 cm, and soil moisture to be set as 0.2 $cm^3\ cm^{-3}$. The correlation function type is found to be fit for the exponential one, from the analysis of in situ roughness measurements (Table 2).

Through statistical analysis, the simulated data were better fitted by a cubic polynomial function, which is expressed as

$$Zs = -0.0009(\Delta\sigma_{IS1-IS7})^3 + 0.0142(\Delta\sigma_{IS1-IS7})^2 - 0.0813(\Delta\sigma_{IS1-IS7}) + 0.3545 \tag{11}$$

where, $\Delta\sigma_{IS1-IS7}$ means the difference in backscattering coefficient for HH polarization. As shown in Fig. 4, this function fits the simulation data well with the coefficient of determination (R^2) nearly equals to 0.94. Accordingly, distributed *Zs* information can be obtained based on a pair of ASAR images with different swaths. Small values of *Zs* correspond to smooth conditions, which often manifest as small values of σ and/or large values of *cl*. In contrast, large values of *Zs* represent rough surfaces.

Additionally, Baghdadi et al. (2006b) provides a calibrated relationship between *cl* and σ obtained from various SAR instrumental configurations, which is

$$cl(\sigma,\theta,pp) = \delta(\sin\theta)^{\mu}\sigma^{(\eta\theta+\xi)} \tag{12}$$

The parameters δ and ζ depend on the polarization, while μ and η were found to be independent of the polarization. All of them are functions of incident angle. By specifying an incidence angle of 43.9° at an HH polarization, the values of these parameters can be obtained using the functions given by Baghdadi et al. (2006b). The relationship between *cl* and σ is then obtained as

$$cl = 7.62\sigma^{1.44} \tag{13}$$

HESSD
7, 3365–3396, 2010

Substituting Eq. (13) into Eq. (11) with the combination of Eq. (9), σ and cl can be calculated for every pixel. As an example, the distribution of the standard deviation of surface height is shown in Fig. 5. It can be noted from the results that most of the experimental area is characterized by moderate or relatively rough surface conditions.

After obtaining the roughness, the soil moisture distribution of the study area was then estimated using the inversion procedure described in Sect. 2.2. Results are illustrated in Fig. 6. The dominant yellow colors in the map represent low levels of soil moisture, in accordance with bare soils. The blue colors correspond to higher soil water content and appeared mainly in vegetated areas. The spatial pattern of mv distribution is reasonable, agreeing well with the local situation because an irrigation was took place just several days ago so the vegetated areas were still wet but the bare areas have turned into dry condition due to very strong evaporation in this arid region.

3.2 Validation

Soil moisture validation was performed at sites D and E. As shown in Fig. 7, the quantifications of mv estimation without eliminating the vegetation effect are also used for comparison. Thus, two groups of scatter points were plotted in each diagram, i.e., before and after the correction of canopy interference for each study site. The results showed that for site D, the root mean square error (RMSE) and the mean error (ME) of mv after the correction of vegetation effect are 0.04 and −0.02, respectively. For site E, the RMSE and the ME of mv after the correction of vegetation effect are 0.06 and −0.03, respectively, manifesting that the results at both sites are a bit underestimated. The correlation coefficient (R) between the observed and estimated soil moisture values at sites D and E are 0.70 and 0.35, respectively. Compared the RMSEs and the correlation coefficients, it is indicated that the results at site D are better than those at site E. This might due to that (1) the canopy is much thicker at site E and (2) the site D is more homogeneous than site E.

HESSD
7, 3365–3396, 2010

3.3 Vegetation effect

The results indicate that the vegetation has a very significant effect on soil moisture estimation. For site D, the RMSE and the ME of *mv* without correcting the vegetation effect are 0.06 and −0.03, respectively. For site E, the two values are 0.14 and −0.12, respectively. It is evident that the thin canopy (alfalfa stubble) at site D does not apparently impact *mv* estimations but the thicker canopy presented at site E could yield more extinction to microwave energy and result in a significant underestimation of *mv*.

Obviously, the canopy effect should be minimized in order to guarantee the applicability of the AIEM. The parameter values of A, b and vwc, are all important for using the water cloud model to correct the vegetation effect. Usually, A and b can be calibrated from observations but not available in this study. An sampling of vwc did occur at site E, but preceded the SAR data collection about nearly 10 days. Thus, these parameters used in vegetation correction are mainly derived form literatures or determined from local situations. It is suggested that although the *mv* estimates were improved after using the water cloud model, it seems that more satisfied results could be obtained using some sophisticated vegetation models or adequate vegetation measurements.

3.4 Error analysis

It also can be seen in Fig. 7 that both at sites D and E, the estimated values of *mv* are lower than those measured in situ. It is suggested that this is partially caused by the difference of sensing depth for soil media between remote sensing and in situ instrumentation. Radar signals in C band essentially perceives the dielectric properties of the superficial soil layer (usually less than 1 cm). On the contrary, for TDR or gravimetric sampling methods, the detected *mv* is the integral value through the entire sampling depth (~5 cm) in the measured soil volume. The uppermost layer of soil is usually drier than deeper layers, especially in arid region. This probably can explain the underestimation of *mv* but needs to be testified in future field experiment.

Furthermore, we are quite aware that some biases in the results can be attributed to the method used to acquire roughness parameters. Equation (12), which is crucial to the derivation of σ and *cl*, is an optimum calibration that inherently depends on the selection of samples and study sites. In spite of the fact that a large quantity of images and corresponding in situ measurements were involved in the deduction of the coefficients used in Eq. (12), it is conceivable that this empirical relationship could contribute more or less errors when it is deployed in our study environment. Uncertainties also arise from the definition of Eq. (11), primarily in two aspects:

- The specific form of the function is greatly controlled by the values of the input parameters used in the forward simulations. For example, the expression of the Eq. (11) evidently differs from the one proposed by Zribi and Dechambre (2002). The difference can be attributed to the dissimilar domains of the input roughness parameters values.

- One of the baselines for using the multi-dimensionality method is the land surface properties are assumed to be unchanged over the satellite data acquisition period. Unfortunately, at present, no SAR sensors onboard satellite platforms have been able to simultaneously offer multi-angular measurements. Thus, it is indispensable to pay attention to the variations in *mv* in cases where radar observations are collected from different dates. Although the temporal gap of the images being used in this study is very short, it is doubtable that it still could result in some uncertainties.

Besides, it is notable that most areas of the FEA, especially bare soils, were suffering from strong salinization, which could result in a non-negligible impact on the soil dielectric properties. Appropriate correction of this type of dielectric constant change, although not the focus of this paper, will need to be quantitatively addressed in future research.

4 Conclusions

Previous studies have demonstrated that it is still problematic to accurately assess soil moisture using theorized models, e.g., IEM or AIEM, if the surface roughness is not appropriately quantified. Conventionally, areal roughness can be obtained from parameterization, ancillary datasets, or by upscaling point measurements. Although these methods are practicable in some way, it is still worthwhile to seek a direct way of quantifying the spatial distribution of roughness at the pixel scale.

This investigation presented in the paper proposed an operational method to simultaneously estimate surface roughness and soil moisture without auxiliary information. It combines an empirical approach to derive roughness, both the standard deviation of surface height and the correlation length, from multi-angular SAR observations, and a physically-based approach to inverse soil moisture from AIEM. An evaluation was carried out in the middle reaches of the Heihe River Basin. The results showed that this method is feasible to extract surface roughness parameters and to estimate soil moisture at an acceptable accuracy (RMSE$<0.06\,\mathrm{cm}^3\,\mathrm{cm}^{-3}$). In addition, the soil moisture estimation was improved after the correction of vegetation impact, e.g., the RMSE was reduced from 0.06 to 0.04 and from 0.14 to 0.06 for sites D and E, respectively. It is suggested that the errors of the estimation can be attributed to the the presence of vegetation, the empirical deduction of surface roughness, the difference in sensing depths between SAR and TDR probe measurements, and the impact of the saline-alkali soils on SAR signals.

In summary, the proposed method is shown to be an effective method for surface roughness characterization and soil moisture mapping at regional scale, based solely on satellite data in place of using ancillary information, such as point measurements by pin-profilometer. Therefore, not only time and resources can be saved, the uncertainties in association with the upscaling of point roughness measurement can be avoided as well.

Potential future works in this aspect could depend on some state-of-the-art tools. With more and more satellites carrying payloads of polarimetric SAR (PolSAR), such as ALOS-PALSAR, Radarsat-2, and TerraSAR constellation, the usage of the polarimetric-decomposition technique to benefit soil moisture derivation can be anticipated. This technique facilitates the separation of the scattering signature into different parts attributed to different objective properties in order to obtain the exclusive contribution of soils underlying canopy layer (Hajnsek et al., 2009). Furthermore, airborne 3-D light detection and ranging (LIDAR) systems may make it possible to effectively collect surface roughness information over large areas, thereby solving the problem of acquiring statistically representative surface roughness measurements. Such a development would dramatically conduce to the inversion of soil moisture (Wagner and Pathe, 2004).

Acknowledgements. This work is supported by the Chinese Academy of Sciences Action Plan for West Development Project “Watershed Allied Telemetry Experimental Research (WATER)” (grant number KZCX2-XB2-09), the NSFC (National Science Foundation of China) projects (grant numbers: 40925004 and 40771036), and the national high-tech program (863) project “A Common Software for Multi-Source Remote Sensing Data Assimilation” (grant number 2009AA12Z130). The authors would also like to thank ESA for the provision of ASAR data in the framework of the Dragon 2 program (Project ID 5322). Special thanks are extended to all crew members at the field campaigns.

References

Álvarez-Mozos, J., González-Audícana, M., Casali, J., and Larrañaga, A.: Effective versus measured correlation length for radar-based surface soil moisture retrieval, Int. J. Remote Sen., 29, 5397–5408, doi:10.1080/01431160802036367, 2008.

Attema, E. P. and Ulaby, F. T.: Vegetation modeled as a water cloud, Radio Sci., 13, 357–364, 1978.

Baghdadi, N., King, C., Chanzy, A., and Wigneron, J. P.: An empirical calibration of the integral

equation model based on SAR data, soil moisture and surface roughness measurement over bare soils, Int. J. Remote Sen., 23, 4325–4340, doi:10.1080/01431160110107671, 2002.
Baghdadi, N., Gherboudj, I., Zribi, M., Sahebi, M., King, C., and Bonn, F.: Semi-empirical calibration of the IEM backscattering model using radar images and moisture and roughness field measurements, Int. J. Remote Sen., 25, 3593–3623, doi:10.1080/01431160310001654392, 2004.
Baghdadi, N., Holah, N., and Zribi, M.: Soil moisture estimation using multi-incidence and multi-polarization ASAR data, Int. J. Remote Sen., 27, 1907–1920, doi:10.1080/01431160500239032, 2006a.
Baghdadi, N., Holah, N., and Zribi, M.: Calibration of the integral equation model for SAR data in C-band and HH and VV polarizations, Int. J. Remote Sen., 27, 805–816, doi:10.1080/01431160500212278, 2006b.
Baghdadi, N., Cerdan, O., Zribi, M., Auzet, V., Darboux, F., Hajj, M. El, and Kheir, R. B.: Operational performance of current synthetic aperture radar sensors in mapping soil surface characteristics: application to hydrological and erosion modelling, Hydrol. Process., 22, 9–20, doi:10.1002/hyp.6609, 2008.
Bindlish, R. and Barros, A. P.: Multifrequency soil moisture inversion from SAR measurements with the use of IEM, Remote Sens. Environ., 71, 67–88, 2000.
Bindlish, R. and Barros, A. P.: Parameterization of vegetation backscatter in radar-based, soil moisture estimation, Remote Sens. Environ., 76, 130–137, 2001.
Bryant, R., Moran, M. S., Thoma, D. P., Collins, C. D., Skirvin, S., Rahman, M., Slocum, K., Starks, P., Bosch, D., and Dugo, M. P.: Measuring surface roughness height to parameterize Radar backscatter models for retrieval of surface soil moisture, IEEE T. Geosci. Remote S., 4, 137–141, doi:10.1109/LGRS.2006.887146, 2007.
Chen, K. S., Wu, T. D., Tsang, L., Li, Q., Shi, J., and Fung, A. K.: Emission of rough surfaces calculated by the integral equation method with comparison to three-dimensional moment method simulations, IEEE T. Geosci. Remote., 41, 90–101, 2003.
Davidson, M. W., Toan, T. L., Mattia, F., Satalino, G., Manninen, T., and Borgeaud, M.: On the characterization of agricultural soil roughness for radar remote sensing studies, IEEE T. Geosci. Remote., 38, 630–640, 2000.
Dobson, M. C., Ulaby, F. T., Hallikainen, M. T., and El-rayes, M. A.: Microwave dielectric behavior of wet soil-part II: dielectric mixing models, IEEE T. Geosci. Remote., GE-23, 35–46, 1985.

HESSD
7, 3365–3396, 2010

Estimation of surface soil moisture and roughness

S. G. Wang et al.

Dubois, P. C., Zyl, J. V., and Engman, T.: Measuring soil moisture with imaging radars, IEEE T. Geosci. Remote., 33, 915–926, 1995.
D'Urso, G. and Minacapilli, M.: A semi-empirical approach for surface soil water content estimation from radar data without a-priori information on surface roughness, J. Hydrol., 321, 297–310, doi:10.1016/j.jhydrol.2005.08.013, 2006.
Fung, A. K., Li, Z., and Chen, K. S.: Backscattering from a randomly rough dielectric surface, IEEE T. Geosci. Remote., 30, 356–369, 1992.
Fung, A. K.: Microwave scattering and emission models and their applications, Artech House Inc., Norwood, MA, 1994.
Hajnsek, I., Jagdhuber, T., Schon, H., and Papathanassiou, K. P.: Potential of estimating soil moisture under vegetation cover by means of PolSAR, IEEE T. Geosci. Remote., 47, 442–454, doi:10.1109/TGRS.2008.2009642, 2009.
Holah, N., Baghdadi, N., Zribi, M., Bruand, A., and King, C.: Potential of ASAR/ENVISAT for the characterization of soil surface parameters over bare agricultural fields, Remote Sens. Environ., 96, 78–86, doi:10.1016/j.rse.2005.01.008, 2005.
Jackson, T. J., Gasiewski, A. J., Oldak, A., Klein, M., Njoku, E., Yevgrafov, A., Christiani, S., and Bindlish, R.: Soil moisture retrieval using the C-band polarimetric scanning radiometer during the southern great plains 1999 experiment, IEEE T. Geosci. Remote., 40, 2151–2161, 2002.
Jackson, T. J., Le Vine, D. M., Swift, C. T., Schmugge, T. J., and Schiebe, F. R.: Large area mapping of soil moisture using the ESTAR passive microwave radiometer in Washita'92, Remote Sens. Environ., 54, 27–37, 1995.
Kerr, Y. H., Waldteufel, P., Wigneron, J. P., Martinuzzi, J. M., Font, J., and Berger, M.: Soil moisture retrieval from space: the soil moisture and ocean salinity (SMOS) mission, IEEE T. Geosci. Remote., 39, 1729–1735, 2001.
Li, X., Li, X., Li, Z., Ma, M., Wang, J., Xiao, Q., Liu, Q., Che, T., Chen, E., Yan, G., Hu, Z., Zhang, L., Chu, R., Su, P., Liu, Q., Liu, S., Wang, J., Niu, Z., Chen, Y., Jin, R., Wang, W., Ran, Y., Xin, X., and Ren, H.: Watershed Allied Telemetry Experimental Research, J. Geophys. Res., 114, D22103, doi:10.1029/2008JD011590, 2009.
Lievens, H., Vernieuwe, H., Álvarez-Mozos, J., De Baets, B., and Verhoest, N. E.: Error in radar-derived soil moisture due to roughness parameterization: an analysis based on synthetical surface profiles, Sensors, 9, 1067–1093, doi:10.3390/s90201067, 2009.
Loew, A., Ludwig, R., and Mauser, W.: Derivation of surface soil moisture from ENVISAT ASAR

wide swath and image mode data in agricultural areas, IEEE T. Geosci. Remote., 44, 889–899, doi:10.1109/TGRS.2005.863858, 2006.
Moran, M. S., Peters-Lidard, C. D., Watts, J. M., and McElroy, S.: Estimating soil moisture at the watershed scale with satellite-based radar and land surface models, Can. J. Remote Sen., 30, 1–22, 2004.
Njoku, E. G. and Entekhabi, D.: Passive microwave remote sensing of soil moisture, J. Hydrol., 184, 101–129, 1996.
Njoku, E. G., Jackson, T. J., Lakshmi, V., Chan, T. K., and Nghiem, S. V.: Soil moisture retrieval from AMSR-E, IEEE T. Geosci. Remote., 41, 215–229, 2003.
Oh, Y., Sarabandi, K., and Ulaby, F. T.: An empirical model and an inversion technique for radar scattering from bare soil surfaces, IEEE T. Geosci. Remote., 30, 370–381, 1992.
Oh, Y., Sarabandi, K., and Ulaby, F. T.: Semi-empirical model of the ensemble-averaged differential Meuller matrix for microwave backscattering from bare soil surfaces, IEEE T. Geosci. Remote., 40, 1348–1355, 2002.
Rahman, M. M., Moran, M. S., Thoma, D. P., Bryant, R., Sano, E. E., Holifield Collins, C. D., Skirvin, S., Kershner, C., and Orr, B. J.: A derivation of roughness correlation length for parameterizing radar backscatter models, Int. J. Remote Sen., 28, 3995–4012, doi:10.1080/01431160601075533, 2007.
Rahman, M. M., Moran, M. S., Thoma, D. P., Bryant, R., Holifield Collins, C. D., Jackson, T. J., Orr, B. J., and Tischler, M.: Mapping surface roughness and soil moisture using multi-angle radar imagery without ancillary data, Remote Sens. Environ., 112, 391–402, doi:10.1016/j.rse.2006.10.026, 2008.
Shi, J., Wang, J., Hsu, A. Y., O'Neill, P. E., and Engman, E. T.: Estimation of bare surface soil moisture and surface roughness parameter using L-band SAR image data, IEEE T. Geosci. Remote., 35, 1254–1266, 1997.
Su, Z., Troch, P. A., and De Troch, F. P.: Remote sensing of bare surface soil moisture using EMAC/ESAR data, Int. J. Remote Sen., 18, 2105–2124, 1997.
Ulaby, F. T., Moore, R. K., and Fung, A. K.: Microwave remote sensing: active and passive, Vol. II – radar remote sensing and surface scattering and rmission theory, Addison-Wesley, Advanced Book Program, Reading, Massachusetts, 609 pp, 1982.
Ulaby, F. T., Moore, R. K., and Fung, A. K.: Microwave remote sensing: active and passive, Vol. III – volume scattering and emission theory, advanced systems and applications, Artech House, Inc., Dedham, Massachusetts, 1100 pp., 1986.

HESSD
7, 3365–3396, 2010

Estimation of surface soil moisture and roughness

S. G. Wang et al.

Verhoest, N., Lievens, H., Wagner, W., Álvarez-Mozos, J., Moran, M. S., and Mattia, F.: On the soil roughness parameterization problem in soil moisture retrieval of bare surfaces from synthetic aperture radar, Sensors, 8, 4213–4248, doi:10.3390/s8074213, 2008.

Wagner, W. and Pathe, C.: Has SAR failed in soil moisture retrieval?, ENVISAT & ERS Symposium, Salzburg, Austria, 6–10 September 2004, ESA SP-572, 1745–1751, 2004.

Wigneron, J. P., Calvet, J. C., Pellarin, T., Van de Griend, A. A., Berger, M., and Ferrazzoli, P.: Retrieving near surface soil moisture from microwave radiometric observations: Current status and future plans, Remote Sens. Environ., 85, 489–506, doi:10.1016/S0034-4257(03)00051-8, 2003.

Wigneron, J.P., Kerr, Y., Waldteufel, P., Saleh, K., Escorihuela, M.J., Richaume, P., Ferrazzoli, P., Rosnay, P. D., Gurney, R., Calvet, J. C., Grant, J., Guglielmetti, M., Hornbuckle, B., Mätzler, C., Pellarin, T., and Schwank, M.: L-band microwave emission of the biosphere (L-MEB) model: description and calibration against experimental data sets over crop fields, Remote Sens. Environ., 107, 639–655, doi:10.1016/j.rse.2006.10.014, 2007.

Wu, T. D., Chen, K. S., Shi, J., and Fung, A. K.: A transition model for the reflection coefficient in surface scattering, IEEE T. Geosci. Remote., 39, 2040–2050, 2001.

Zribi, M., Baghdadi, N., and Guérin, C.: Analysis of surface roughness heterogeneity and scattering behavior for radar measurements, IEEE T. Geosci. Remote., 44, 2438–2444, doi:10.1109/TGRS.2006.873742, 2006.

Zribi, M., Baghdadi, N., Holah, N., Fafin, O., and Guérin, C.: Evaluation of a rough soil surface description with ASAR-ENVISAT radar data, Remote Sens. Environ., 95, 67–76, doi:10.1016/j.rse.2004.11.014, 2005.

Zribi, M. and Dechambre, M.: A new empirical model to retrieve soil moisture and roughness from C-band radar data, Remote Sens. Environ., 84, 42–52, 2002.

Table 1. Ground truth measurements of soil moisture and surface roughness.

site	In situ measurement					
	mv (cm^3 cm^{-3}) (06/27/2008)			σ (cm)		
	range	mean	standard deviation	range	mean	standard deviation
A	0.23~0.54	0.39	0.08	1.11~2.09	1.51	0.31
B	0.13~0.42	0.28	0.05	0.68~4.08	1.40	0.53
C		N/A		0.58~4.46	1.28	0.66
D	0.02~0.20	0.09	0.05			N/A
E	0.08~0.34	0.25	0.05			N/A

HESSD
7, 3365–3396, 2010

Table 2. Summary of the parameter values used in the Dobson dielectric mixing model and the AIEM.

Parameters	Value		
f (GHz)	5.3		
θ (°)	18.4, 28.5, 43.9		
Initial value of mv ($cm^3\,cm^{-3}$)	0.2		
Land surface temperature T (°)	27		
Soil density ($g\,cm^{-3}$)	specific density		bulk density
	2.70		1.31
Soil porosity	0.51		
Soil texture (%)	sand		clay
	20.5		8.5
σ (cm)	min	max	increment
	0.3	3.0	0.1
cl (cm)	min	max	increment
	3	35	2
Correlation function type	exponential		

HESSD
7, 3365–3396, 2010

Estimation of surface soil moisture and roughness

S. G. Wang et al.

Table 3. Vegetation parameters used in the water cloud model.

site	*A*	*b*	vwc ($kg\,m^{-2}$)	land cover
D	0.01	0.084	0.3	alfalfa after harvest
E	0.05	0.3	1.46	barley in mature stage

HESSD

7, 3365–3396, 2010

Estimation of surface soil moisture and roughness

S. G. Wang et al.

Table 4. List of ASAR images used in this study.

ASAR images			
Date	Polarization	Swath	Central lat/long (degree)
06/25/2008	HH/HV	IS3, 28.5°	38.97/100.23
06/27/2008	HH/HV	IS7, 43.9°	38.97/100.08
06/28/2008	HH/HV	IS1, 18.4°	38.89/100.48

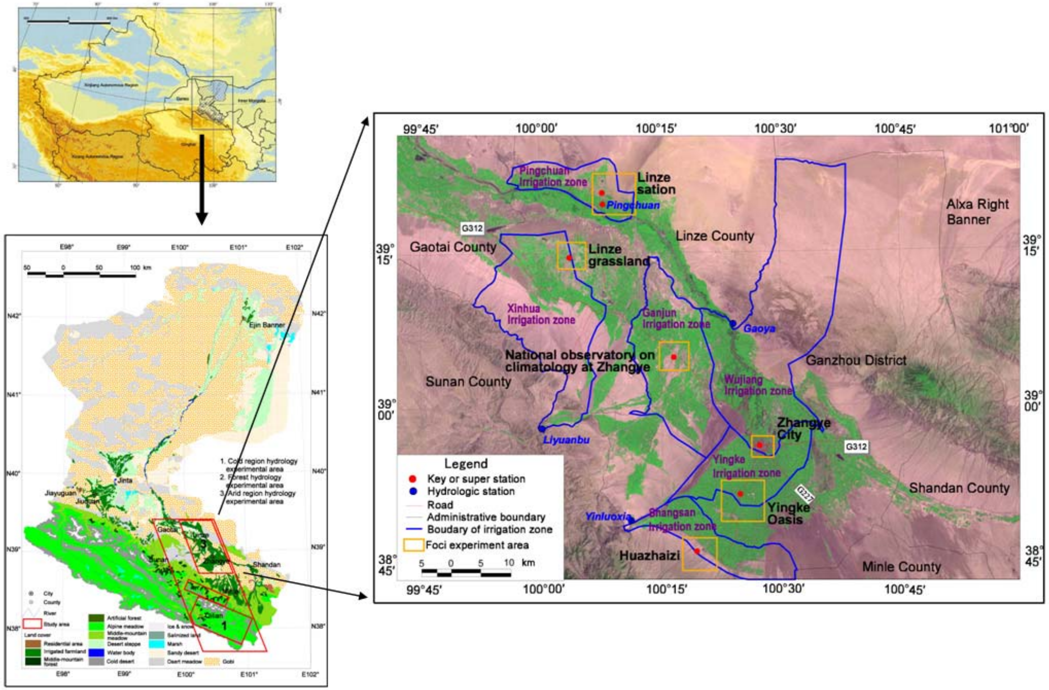

Fig. 1. Location of the Linze grassland (LZG; upper left yellow square) in the arid region hydrology experiment (ARHE; right picture) in the Heihe river basin (bottom left picture).

HESSD
7, 3365–3396, 2010

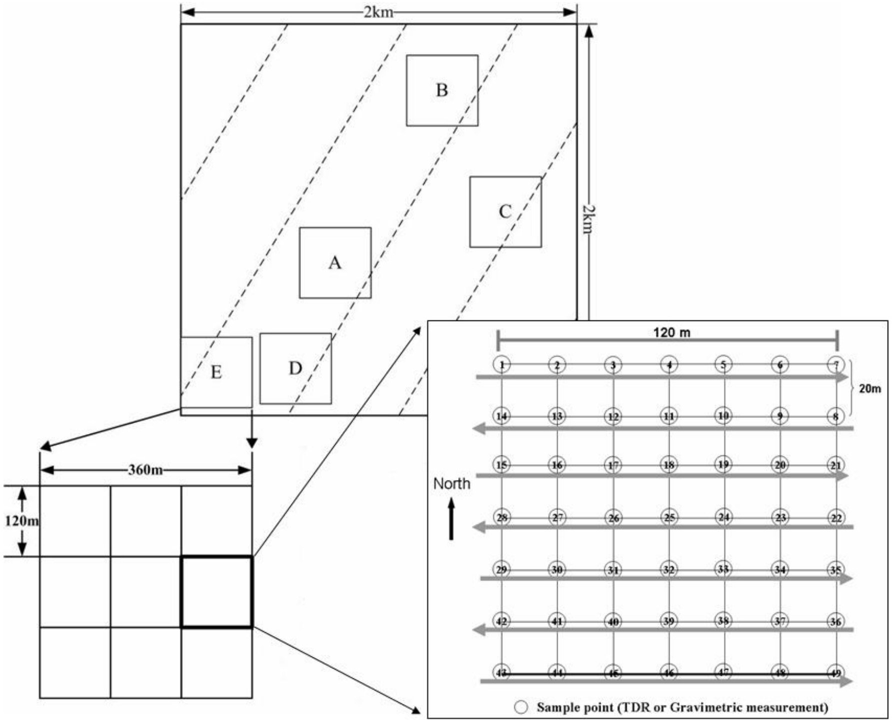

Fig. 2. The three-level soil moisture sampling strategy designed for use in field campaigns. Resolution ranges from coarse to fine, corresponding to the foci experimental area, experimental site, and elementary sampling plot.

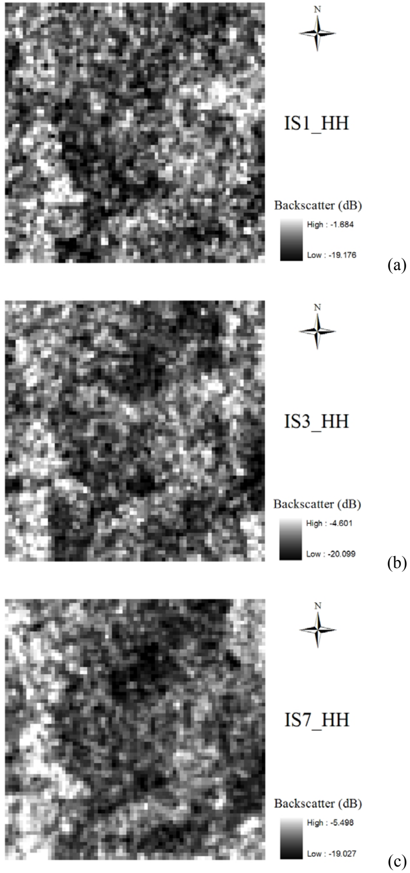

Fig. 3. Segment scenes of processed multi-angular images in the region of the study area (**(a)**, **(b)**, and **(c)** correspond to IS1, IS3, and IS7 swaths, respectively).

HESSD
7, 3365–3396, 2010

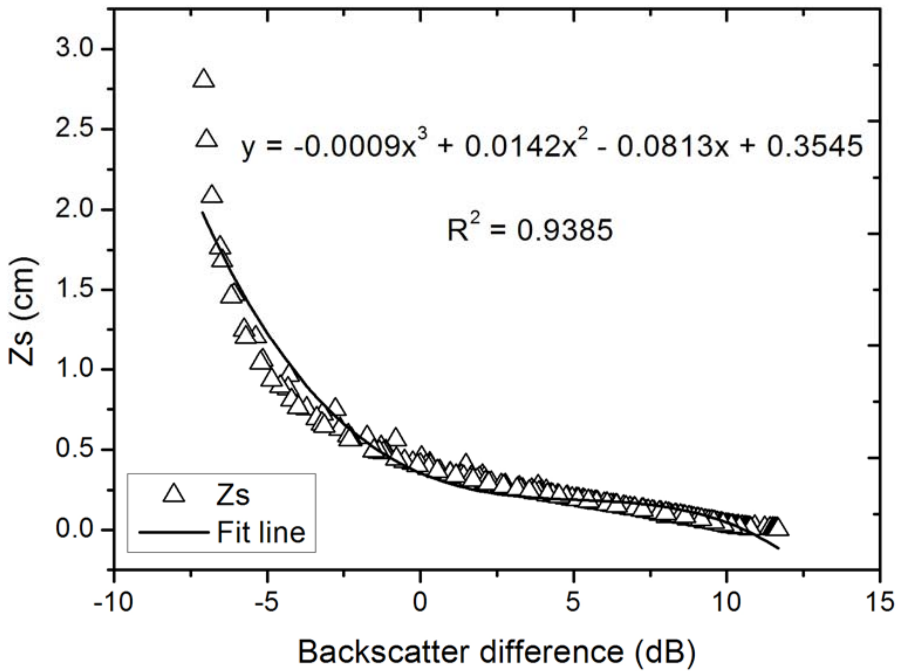

Fig. 4. Sketch map of the relationship between *Zs* and $\Delta\sigma_{IS1-IS7}$ (incidence angles of 18.5° and 43.9°) provided by Eq. (11).

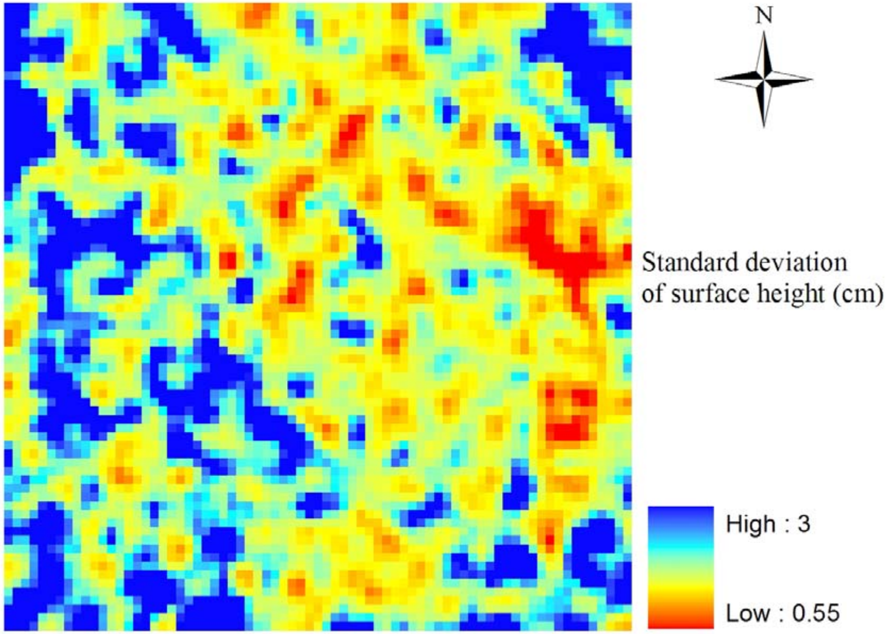

Fig. 5. Estimated result of standard deviation of surface height based on two images with swath modes of *IS*1 and *IS*7 in association with Eqs. (9)–(13).

HESSD
7, 3365–3396, 2010

Estimation of surface soil moisture and roughness

S. G. Wang et al.

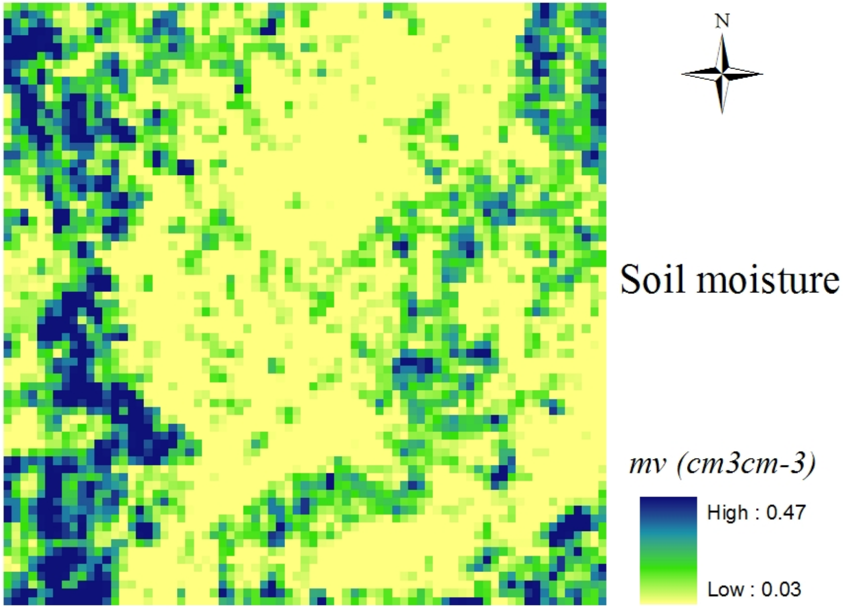

Fig. 6. Retrieved mv in the study area based on the results of the surface roughness acquired by the proposed multi-angular algorithm.

HESSD
7, 3365–3396, 2010

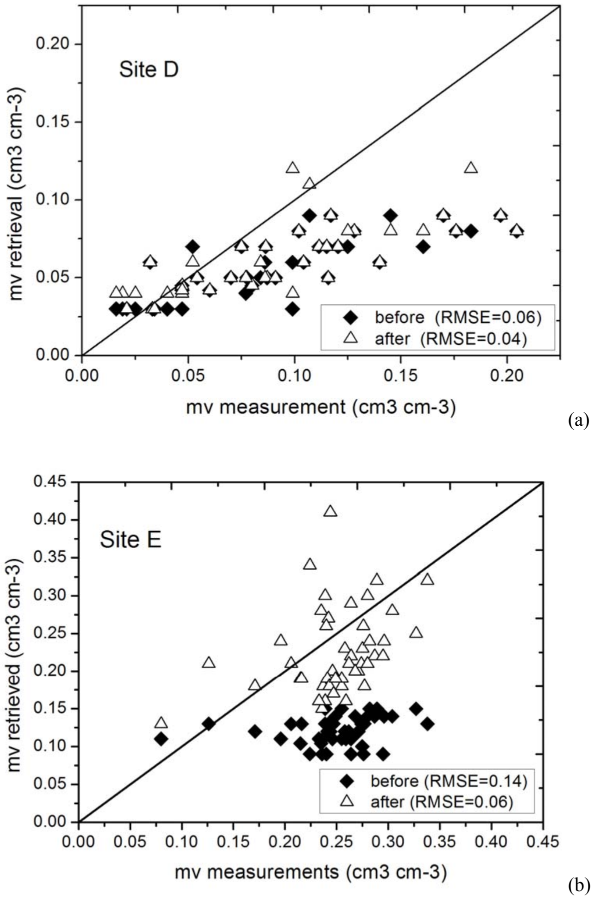

Fig. 7. Comparison between mv estimated from radar imagery and from in situ measurements at **(a)** site D and **(b)** site E before vegetation correction (before, ♦) and after elimination of the canopy effect (after, Δ).

HESSD
7, 3365–3396, 2010

Estimation of surface soil moisture and roughness

S. G. Wang et al.